Interference with Immunoglobulin (Ig)α Immunoreceptor Tyrosine–based Activation Motif (ITAM) Phosphorylation Modulates or Blocks B Cell Development, Depending on the Availability of an Igβ Cytoplasmic Tail

Manfred Kraus,[1] Lily I. Pao,[1] Amy Reichlin,[2] Yun Hu,[2] Beth Canono,[3] John C. Cambier,[3] Michel C. Nussenzweig,[2] and Klaus Rajewsky[1]

[1]*Institute for Genetics, University of Cologne, D-50931 Cologne, Germany*
[2]*Laboratory of Molecular Immunology, The Rockefeller University and the Howard Hughes Medical Institute, New York, NY 10021*
[3]*Integrated Department of Immunology, University of Colorado Health Sciences Center and National Jewish Medical and Research Center, Denver, CO 80206*

Abstract

To determine the function of immunoglobulin (Ig)α immunoreceptor tyrosine–based activation motif (ITAM) phosphorylation, we generated mice in which Igα ITAM tyrosines were replaced by phenylalanines ($Ig\alpha^{FF/FF}$). $Ig\alpha^{FF/FF}$ mice had a specific reduction of B1 and marginal zone B cells, whereas B2 cell development appeared to be normal, except that λ1 light chain usage was increased. The mutants responded less efficiently to T cell–dependent antigens, whereas T cell–independent responses were unaffected. Upon B cell receptor ligation, the cells exhibited heightened calcium flux, weaker Lyn and Syk tyrosine phosphorylation, and phosphorylation of Igα non-ITAM tyrosines. Strikingly, when the Igα ITAM mutation was combined with a truncation of Igβ, B cell development was completely blocked at the pro-B cell stage, indicating a crucial role of ITAM phosphorylation in B cell development.

Key words: mb-1 protein • B cell antigen receptor • ITAM • B cell subsets • gene targeting

Introduction

B cell development is a highly ordered and controlled process allowing the formation of a diverse repertoire of B cell receptor (BCR)* antigen specificities. Dependent on the developmental status and the microenvironment of the B cell, the strength and quality of BCR transmitted signals control survival, differentiation, and proliferation (1, 2).

The BCR is a multimeric protein complex consisting of an antigen binding module that is noncovalently associated with one signal-transducing heterodimer of Igα (CD79a, mb-1) and Igβ (CD79b, B29) (3). An early and essential feature of the signaling cascade is phosphorylation of the tyrosine residues within immunoreceptor tyrosine–based activation motif (ITAM) by Src family protein tyrosine kinases (PTKs; references 4, 5, and 6). The phosphorylated ITAMs are thought to serve as docking sites for Src homology 2 (SH2) domain–containing proteins. For instance, dual phosphorylation of the BCR ITAMs allows high affinity association of the tandem SH2 domain–containing kinase Syk. Binding of Syk to ITAM leads to its phosphorylation and activation which in turn leads to phosphorylation of downstream cellular substrates. Igα and Igβ both contain single ITAMs that potentially confer distinct signaling functions. In support of this idea, several proteins have been shown to associate differentially with either Igα or Igβ (7, 8). In transfection experiments using chimeric molecules, isolated cytoplasmic domains of either Igα or Igβ were both capable of mediating the mobilization of calcium and tyrosine phosphorylation of cellular molecules. These signaling capacities were critically dependent on ITAM phosphorylation. Further data suggest that Igα is predominant in activating PTKs (9–16).

K. Rajewsky's present address is Center for Blood Research, Harvard Medical School, 200 Longwood Ave., Boston, MA 02115.

Address correspondence to Manfred Kraus at his present address Center for Blood Research, Harvard Medical School, 200 Longwood Ave., Boston, MA 02115. Phone: 617-278-3274; Fax: 617-278-3131; E-mail: kraus@cbr.med.harvard.edu

**Abbreviations used in this paper:* BCR, B cell receptor; BM, bone marrow; ES, embryonic stem; ITAM, immunoreceptor tyrosine–based activation motif; MZ, marginal zone; PTK, protein tyrosine kinase; RT, room temperature; SH2, Src homology 2; TD, T cell–dependent; TI, T cell–independent.

Aspects of Igα and Igβ function in B cell development were studied in transgenic and gene-targeted mice. In Igβ knockout mice, the lack of Igα/Igβ heterodimer formation presumably also abrogates the surface expression of Igα and results in a complete block of development at the pro-B cell stage (17). However, the expression of chimeric molecules with cytoplasmic domains of either Igα or Igβ was capable of supporting further steps in B cell maturation, including H chain allelic exclusion (18–20). Critical roles of the cytoplasmic tails of Igα and Igβ in B cell development were revealed in *mb-1*$^{\Delta c/\Delta c}$ and *Igβ*$^{\Delta c/\Delta c}$ mice (21, 22). In *Igβ*$^{\Delta c/\Delta c}$ mice, the cytoplasmic domain of Igβ is lacking, whereas in *mb-1*$^{\Delta c/\Delta c}$ mice (hereafter termed *Igα*$^{\Delta c/\Delta c}$) a truncated Igα protein with a cytoplasmic domain consisting of 20 instead of 61 amino acids is expressed. In both mutants, B cell development is severely impaired resulting in a drastic reduction of peripheral B lymphocyte numbers. Functionally, the remaining B cells in the mutants are unable of mounting a measurable immune response against T cell–independent (TI) antigen. Further experiments with *Igα*$^{\Delta c/\Delta c}$ mice revealed that the Igα cytoplasmic truncation causes enhanced negative selection of autoreactive receptor specificities and generally renders immature B cells more sensitive to antigenic contact. Based on these data, an additional negative signaling function for Igα was suggested (23, 24).

To investigate the specific function of Igα ITAM phosphorylation in B cell development, we generated a mutant mouse strain by gene targeting in which the Igα ITAM tyrosines were replaced with phenylalanines (*Igα*$^{FF/FF}$ mice).

Materials and Methods

Generation of Targeting Vector and Targeted Embryonic Stem Cell Clones. The *mb-1* targeting vector was designed as a replacement vector (25). A loxP site was inserted into the Tth111I site of intronIII. Intronic region and exons downstream of this loxP site are exactly repeated 3′ to a floxed *neo*^{r} gene (see Fig. 1 A). Tyrosine to phenylalanine replacements within the ITAM were achieved by site-directed mutagenesis (Tyr_{182}: TAT to TTC; Tyr_{193}: TAT to TTT). An additional BamHI restriction site within the 3′ UTR, downstream of the mutated exons, was generated by an exchange of two nucleotides.

A 5.2-kb genomic BamHI fragment, containing the *mb-1* gene, was recovered from a murine cosmid (C57BL/6J-pWE15 library; Stratagene; reference 26) and subcloned into the BamHI site of pGEM-7Z+ (Promega) to generate pGEM5.2kbBamHI. Subsequently, a 1.4-kb Tth111I–XhoI fragment was recovered from this vector and subcloned into the EcoRI/XhoI sites of pGEMloxP (unpublished data) to obtain pGEMloxPTth111I-XhoI. Next, the Tth111I–PstI fragment of pGEM5.2kbBamHI was replaced with the NotI–PstI fragment from pGEMloxPTth111I-XhoI to obtain pGEM5.2kbloxP. The 5.2-kb BamHI fragment was then cloned into the BamHI site of pSL1190XX to obtain pSL5.2kbloxP. pSL1190XX was generated from pSL1190 (Amersham Pharmacia Biotech) by deleting the polylinker-region between XhoI and XbaI.

The region downstream of the *mb-1* polyA site was extended 0.4 kb by the following procedure. A 1.2-kb fragment was first amplified by PCR from the genomic cosmid clone with the primers 3′ region-FOR (5′-CTGCCTCCCCACTCTTCC-3′) and 3′ region-REV (5′-CCATCGATCCTGCCGCGGCCGC-TTACTCT-3′). This PCR product was subcloned into the pCR™ TA Cloning vector II (Invitrogen), and a 1.2-kb EcoRI–XhoI fragment was recovered. This fragment was used to replace the 0.8-kb SmaI–XhoI fragment in pSL5.2kbloxP to obtain pSL5.2kbloxP-3′. Next, pSL5.2kbloxP-3′ was cut with EcoRV–XbaI and religated resulting in pSL5.2kbloxP-3′-ΔClaI. Subsequently, the *tk* selection marker was excised as a HindIII fragment from pIC-TKΔCla1, a modified version of pIC19R/MC1-TK (26). This fragment was cloned into the HindIII site of pSL5.2kbloxP-3′-ΔClaI to obtain pSL5.2kbloxP-3′-ΔClaI-TK. For the construction of a loxP-flanked *neo*^{r} cassette, a SalI–XhoI fragment was recovered from pMC1neoPolyA (Stratagene) and cloned into the XhoI site of pGEMloxP to obtain pGEM-neoloxP. From this vector, an XbaI–HindIII fragment was subcloned into NotI–HindIII sites of pGEMloxP, resulting in pMM-neoflox-8. A 1.2-kb XbaI–NsiI fragment from pMMneoflox-8 was cloned into Tth111I–NsiI–digested pGmb1C1C2** (21) to obtain pmb-1C1C2**neoflox. Additional restriction sites were introduced by site-directed mutagenesis. The product of two consecutive PCR reactions (primer: BamHI-FOR 5′-ATGT-CTGGATCCAGCATCCC-3′; BamHI-REV 5′-GGGATGCT-GGATCCAGACAT-3′; FLAG-C1C2**-FOR 5′-AACGGTG-GCAAAATGAGAAG-3′; FLAG-C1C2**-REV 5′-TTGGGC-CCCGATCGATCGCATG-3′) was subcloned into the pCR™ TA Cloning vector II (Invitrogen) and retrieved by digestion with SalI and ApaI. The fragment was used to exchange the corresponding 1-kb fragment in pmb-1C1C2**neoflox to generate pmb-1C1C2**neoflox-BamHI.

Culturing and transfection of E14.1 embryonic stem (ES) cells (129/Ola) was performed according to previously published protocols (27). Screening of 596 G418/gancyclovir double resistant colonies by Southern blot analysis led to the identification of three homologous recombinant ES cell clones (Fig. 1).

Mice. ES cells carrying the *Igα*$^{FF\text{-}Flox}$ allele were injected into C57BL/6 and CB20 blastocysts which were then transferred into foster mothers to obtain chimeric mice. Mice with the *Igα*$^{FF\text{-}Flox}$ allele were crossed to the *deleter*-strain (28). Some analyses were performed with *Igα*$^{FF/FF}$ mice of a mixed 129/Ola–C57BL/6 genetic background. To control for a potential influence of the genetic background (e.g., in immunization studies), control groups of 129/Ola and C57BL/6 mice were included and analyzed in parallel with the *Igα*$^{FF/FF}$ mice. In anti-phosphotyrosine immunoblotting experiments, all *Igα*$^{FF/FF}$ mice used had been backcrossed for eight generations to C57BL/6. *Igβ*$^{\Delta c/\Delta c}$ mice (22) are of mixed 129/Sv–C57BL/6 genetic background. *Igα*$^{\Delta c/\Delta c}$ mice (21) are of C57BL/6 genetic background. *Igα*$^{FF/FF}$*Igβ*$^{\Delta C/\Delta C}$ mice were generated by intercrossing *Igα*$^{FF/FF}$ mice to *Igβ*$^{\Delta C/\Delta C}$ mice (22). All mice, including *Igα*$^{\Delta C/\Delta C}$ (21) and $J_H T/J_H T$ mice (29), were housed in our conventional animal facility.

Preparation of Cell Suspensions from Lymphoid Organs. Spleens were minced through a nylon mesh (cell strainer; Falcon) to obtain single cell suspensions in DMEM, 5% FCS, and 2 mM L-glutamine. Bones were flushed with medium to extract bone marrow (BM) cells and the peritoneal cavity was flushed twice with 10 ml of medium to recover cells. Erythrocytes were lysed from spleen and BM preparations by incubating in lysis buffer (140 mM NH_4Cl, 17 mM Tris-HCl, pH 7.65) for 2 min on ice. To obtain PBLs, mice were bled from the tail vein in the presence of heparin (Liquemin; Roche) and purified by gradient centrifugation with 7% Ficoll 400 (Amersham Pharmacia Biotech).

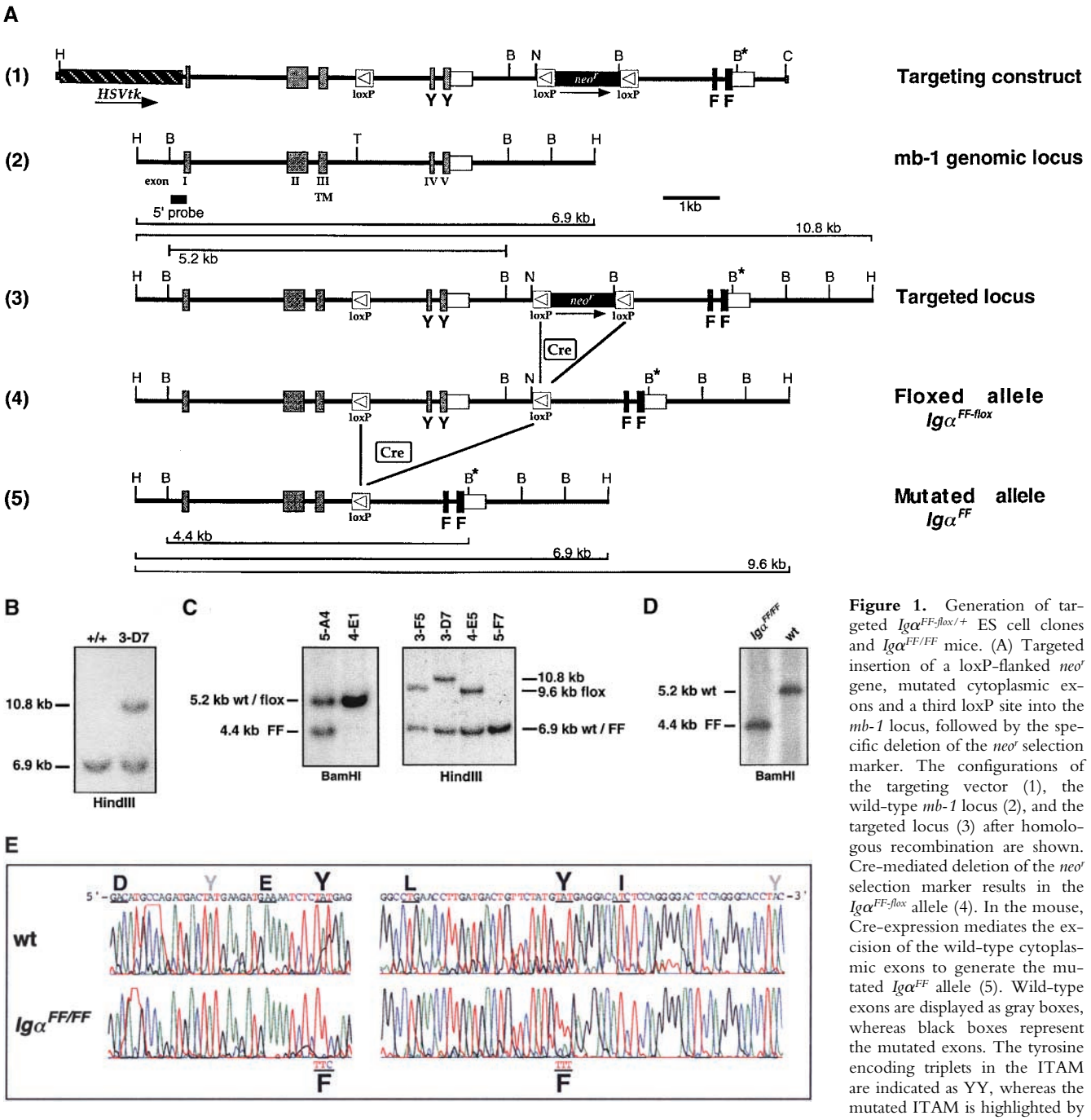

Figure 1. Generation of targeted $Ig\alpha^{FF\text{-}flox/+}$ ES cell clones and $Ig\alpha^{FF/FF}$ mice. (A) Targeted insertion of a loxP-flanked *neo*^{r} gene, mutated cytoplasmic exons and a third loxP site into the *mb-1* locus, followed by the specific deletion of the *neo*^{r} selection marker. The configurations of the targeting vector (1), the wild-type *mb-1* locus (2), and the targeted locus (3) after homologous recombination are shown. Cre-mediated deletion of the *neo*^{r} selection marker results in the $Ig\alpha^{FF\text{-}flox}$ allele (4). In the mouse, Cre-expression mediates the excision of the wild-type cytoplasmic exons to generate the mutated $Ig\alpha^{FF}$ allele (5). Wild-type exons are displayed as gray boxes, whereas black boxes represent the mutated exons. The tyrosine encoding triplets in the ITAM are indicated as YY, whereas the mutated ITAM is highlighted by FF. The white box shows the 3′ UTR, and boxes with a triangle represent loxP sites. Arrows underneath the targeting construct indicate the direction of transcription in the selection marker genes. The map is drawn to scale except for the loxP sites and displays the following restriction sites: B, BamHI; C, ClaI; H, HindIII; N, NotI; T, Tth111I. An asterisk marks the additional BamHI restriction site in the 3′ UTR of the mutated cytoplasmic exons. The external probe used to verify the targeting event is indicated together with the expected sizes of the restriction fragments. (B) Southern blot analysis of ES cell clones after transfection with the targeting construct. Genomic DNA was digested with HindIII and hybridized with the 5′ external probe. The targeted ES cell clone 3-D7, with the characteristic band of 10.8 kb, is shown in comparison to a clone that possesses only the wild-type mb-1 locus (+/+). (C) Southern blot analysis of targeted, G418 sensitive ES cell clones after transient Cre expression. Genomic DNA was digested with either HindIII or BamHI and hybridized with the 5′ external probe. ES cell clones with specific *neo*^{r} deletion (3-F5, 4-E5) show a characteristic band of 9.6 kb after HindIII digestion. Complete deletion of all loxP flanked sequences is characterized by the presence of a 4.4-kb fragment after BamHI digestion (5-A4). For comparison, the parental G418 resistant clone 3-D7 is included in the HindIII based analysis. (D) Southern blot analysis with the 5′ external probe of BamHI digested genomic DNA from $Ig\alpha^{FF/FF}$ and wild-type (wt) mice. (E) Sequence analysis of the Igα ITAM in $Ig\alpha^{FF/FF}$ mice. Genomic DNA was extracted from purified splenic B cells of $Ig\alpha^{FF/FF}$ and wild-type mice. Triplets encoding for the amino acids of the consensus ITAM sequence are underlined and the respective amino acid is indicated. Intronic sequence is not shown (gap). The positions of the two non-ITAM Igα tyrosines are indicated by a gray Y.

Flow Cytometry. Cells were surface stained with combinations of FITC, PE, Cy-Chrome (Cyc), peridinine chlorophyll protein (PERCP), and/or allophycocyanin (APC)-conjugated monoclonal antibodies for 20 min on ice. Stainings with biotinylated monoclonal antibodies were followed by a secondary staining with either Streptavidin-Cy-Chrome (BD PharMingen) or Streptavidin-PERCP (Becton Dickinson). After staining, the samples were washed and resuspended with PBS, 1% BSA, and 0.01% N_3. Stained cells were acquired on a FACScan™ or FACSCalibur™ and data were analyzed using CELLQuest™ software (Becton Dickinson). Dead cells were labeled with propidium iodide or Topro-3 (Molecular Probes) and excluded from the analysis.

For intracellular Igμ chain staining, cells were first washed in PBS then fixed in a 2% formaldehyde solution for 30 min at room temperature (RT). After three washes with PBS, the cells were stained for 20 min at RT with antibody M41 in 0.05% Saponin in PBS. Monoclonal antibodies R33–24.12 (anti-IgM), 1.3–5 (anti-IgD), RA3–6B2 (anti-B220), M41 (anti-μ chain), LS.136 (anti-λ1), Cy34.1 (anti-CD22), M5/114 (anti-MHC class II), BP-1 (anti-BP-1), 30F1 (anti-HSA), and Cfo1 (anti-Thy1.2) were prepared and conjugated in our laboratory. Monoclonal antibodies to CD5, CD19, CD21/CD35, CD23, CD25, CD43, CD69, and CD86 were purchased from BD PharMingen. Anti-493 antibody was a gift from A. Rolink (Basel Institute of Immunology, Basel, Switzerland).

Immunization and Serum Analysis. Mice were immunized with 5 or 50 μg of T cell–dependent (TD) antigen NP-CG (4-hydroxy-3-nitrophenylacetyl chicken-γ-globulin) in alum intraperitoneally. Mice were boosted with 5 μg/200 μl of NP_{17}-CG without adjuvant. TI immune response was analyzed by intraperitoneal injections of 5 μg/200 μl of NP_{27}-Ficoll. Mice were bled before and after immunization from tail veins. Ig serum concentrations were determined by ELISA as described previously (30).

Affinities of IgG1 and λ NP-specific antibodies were determined by calculating the association constant as described previously (31). Briefly, relative binding of serum antibodies to NP_5-BSA versus NP_{14}-BSA was determined by ELISA in comparison to anti-NP antibody standards of known affinity.

Measurement of Ca^{2+} Mobilization. Spleen cells (5×10^6/ml) were loaded with 2 μM Indo-1 AM in RPMI, 2% FCS for 30 min at 37°C (Molecular Probes). Afterwards, the cells were washed and stained with anti–B220-PE (RA3–6B2) monoclonal antibody in RPMI at RT. Fluorescence ratios of Indo-1 emission at 395/510 nm were measured by flow cytometry on a dual laser FACStar™ (Becton Dickinson). Data acquisition was conducted for 50 s without stimulus, followed by the addition of either $F(ab)'_2$ rabbit anti-mouse IgM+G+A fragments (Zymed Laboratories) or rabbit anti–mouse IgM+G+A antibodies (Zymed Laboratories). Data was collected for 512 s and analyzed using CELLQuest™ (Becton Dickinson) and FlowJo (TriStar) software.

Analysis of Protein Tyrosine Phosphorylation. $CD19^+$ B cell populations were purified from splenic cell suspensions by magnetic beads (MACS; Miltenyi Biotec) according to the manufacturer's instructions. B lymphocytes were resuspended at 10^7 cells/ml in RPMI and stimulated with $F(ab)'_2$ rabbit anti–mouse IgM+G+A fragments (Zymed Laboratories) for various time periods at 37°C. The reactions were stopped by addition of ice cold lysis buffer to a final concentration of 1% NP-40, 150 mM NaCl, 0.4 mM EDTA, 10 mM Tris-HCl, pH 8, 1 μg/ml leupeptin, 1 μg/ml aprotinin, 1 μg/ml α1-antitrypsin, 1 mM PMSF, 10 mM sodium pyrophosphate, 2 mM Na_3VO_4, and 10 mM NaF. After incubation on ice for 10 min, lysates were cleared at 12,000 *g* for 5 min at 4°C. Igα was immunoprecipitated from cleared lysates with anti-Igα monoclonal antibody 172 directly coupled to Sepharose beads. For the immunoprecipitation of Lyn or Syk, cleared lysates were incubated with either rabbit polyclonal anti–mouse Lyn (sc-15; Santa Cruz Biotechnology, Inc.) or rabbit polyclonal anti–mouse Syk antibodies (13), respectively; followed by addition of protein G-Sepharose beads (Amersham Pharmacia Biotech). Proteins were resolved by 10% SDS-PAGE, transferred to polyvinylidine difluoride (PVDF) membrane (Millipore), and immunoblotted with anti-phosphotyrosine antibody Py54 (Calbiochem), followed by horseradish peroxidase (HRP)-conjugated rat anti–mouse IgG (Amersham Pharmacia Biotech) and developed by chemiluminescence (ECL; Amersham Pharmacia Biotech). To determine the amount of protein loaded in each lane, the same membranes were stripped and reprobed with appropriate antibodies.

Results

Generation of $Ig\alpha^{FF/FF}$ Mice. To allow for conditional mutation of the Igα ITAM at different stages of B cell development, two *loxP* sites flanking both cytoplasmic exons were targeted into the *mb-1* locus (floxed allele; Fig. 1 A, 4). Downstream of the 3′ end of *mb-1* gene, mutated cytoplasmic exons encoding phenylalanine instead of tyrosine within the ITAM were inserted. Transfection of E14.1 ES cells led to the identification of three homologous recombinant ES cell clones (Fig. 1 A, 3, and Fig. 1 B). One clone (3-D7) was shown by PCR analysis to have cointegrated the 5′ *loxP* site and the ITAM mutations (data not shown). To remove the floxed *neo*^{r} selection cassette from the targeted *mb-1* allele, the clone was transiently transfected with circular pICcre plasmid (29). Resulting G418-sensitive ES cell clones were screened by Southern blot (Fig. 1 C) and PCR analysis (not shown) to distinguish clones that carry the $Ig\alpha^{FF\text{-}flox}$ floxed allele (Fig. 1 A, 4) from clones where Cre-mediated recombination led also to the loss of the unmutated cytoplasmic exons ($Ig\alpha^{FF}$ mutated allele; Fig. 1 A, 5). ES cells carrying the $Ig\alpha^{FF\text{-}flox}$ allele were injected into mouse blastocysts to generate chimeras that subsequently transmitted the floxed allele through the germline. $Ig\alpha^{FF\text{-}flox/+}$ mice were bred with the *deleter* mouse strain (28) to obtain $Ig\alpha^{FF/+}$ mice that were then bred to homozygosity. The tyrosine to phenylalanine exchanges in the Igα ITAM were verified by sequencing. DNA for this analysis was prepared from FACS®-sorted splenic B cells of $Ig\alpha^{FF/FF}$ and wild-type control mice (Fig. 1 E).

B Cell Development in $Ig\alpha^{FF/FF}$ Mice. The requirement of Igα ITAM phosphorylation for B cell development was analyzed in $Ig\alpha^{FF/FF}$ mice by flow cytometry (32). In contrast to $Ig\alpha^{\Delta c/\Delta c}$ mice, which have reduced fractions of pre-B and immature B cells, $Ig\alpha^{FF/FF}$ mice had normal numbers of pro-B ($B220^{low}CD43^+IgM^-$), pre-B ($B220^{low}CD43^-IgM^-$), and immature B ($B220^{low}IgM^+IgD^-$) cells in the BM (Fig. 2 A, and Table I). Similarly, the earliest stages of B cell development within the pro-B cell compartment, fractions A to C′, were not blocked in $Ig\alpha^{FF/FF}$ mice (see Fig. 5). In addition, a striking difference exists between mature B cells in $Ig\alpha^{\Delta c/\Delta c}$ and $Ig\alpha^{FF/FF}$ mutants. Whereas recirculating B

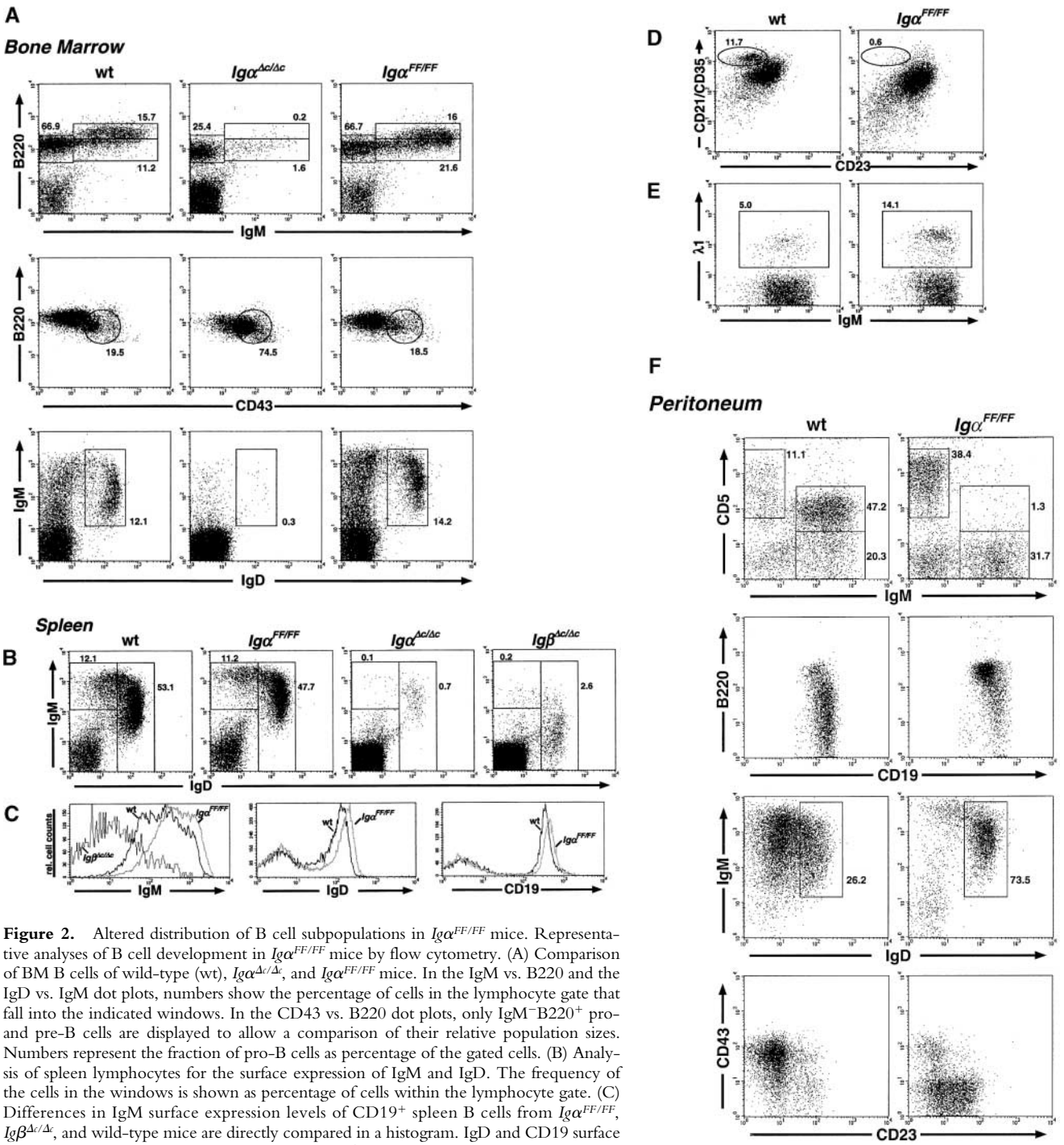

Figure 2. Altered distribution of B cell subpopulations in $Ig\alpha^{FF/FF}$ mice. Representative analyses of B cell development in $Ig\alpha^{FF/FF}$ mice by flow cytometry. (A) Comparison of BM B cells of wild-type (wt), $Ig\alpha^{\Delta c/\Delta c}$, and $Ig\alpha^{FF/FF}$ mice. In the IgM vs. B220 and the IgD vs. IgM dot plots, numbers show the percentage of cells in the lymphocyte gate that fall into the indicated windows. In the CD43 vs. B220 dot plots, only IgM^-B220^+ pro- and pre-B cells are displayed to allow a comparison of their relative population sizes. Numbers represent the fraction of pro-B cells as percentage of the gated cells. (B) Analysis of spleen lymphocytes for the surface expression of IgM and IgD. The frequency of the cells in the windows is shown as percentage of cells within the lymphocyte gate. (C) Differences in IgM surface expression levels of $CD19^+$ spleen B cells from $Ig\alpha^{FF/FF}$, $Ig\beta^{\Delta c/\Delta c}$, and wild-type mice are directly compared in a histogram. IgD and CD19 surface expression levels of spleen lymphocytes of $Ig\alpha^{FF/FF}$ mice are shown in comparison to wild-type controls. (D) Analysis of spleen cells to determine the fraction of MZ B lymphocytes. Shown are $CD19^+$ spleen B lymphocytes; numbers represent $CD21^{high}CD23^{low}$ cells from wild-type (9.9% ± 6.0, $n = 4$; average ± SD) and $Ig\alpha^{FF/FF}$ mice (2.1% ± 1.5; $n = 5$). (E) Fraction of $CD19^+$ spleen B lymphocytes expressing a λ1 light chain. (F) Analysis of peritoneal lymphocytes in $Ig\alpha^{FF/FF}$ mice. In the IgM vs. CD5 dot plot, cells with the forward and side scatter characteristics of lymphocytes are shown. T cells (IgM^-CD5^+): wt 12.3% ± 7.3, $n = 10$; $Ig\alpha^{FF/FF}$ 21.7% ± 10.6, $n = 12$. B cells (IgM^+CD5^+): wt 35.5% ± 11.6, $n = 10$; $Ig\alpha^{FF/FF}$ 3.7% ± 1.6, $n = 12$. (IgM^+CD5^-): wt 38.1% ± 12.5, $n = 10$; $Ig\alpha^{FF/FF}$ 51.7% ± 21.5, $n = 12$. Percentages given are averages ± SD. The other dot plots present surface expression levels of $CD19^+$ peritoneal B lymphocytes from $Ig\alpha^{FF/FF}$ and wild-type mice.

cells in the BM and splenic B cells were ~100-fold reduced in the former, B cell numbers in $Ig\alpha^{FF/FF}$ mice were only marginally reduced in comparison to wild-type mice (Table I; Fig. 2, A and B). We analyzed the peripheral B cells in $Ig\alpha^{FF/FF}$ mice for the expression of several surface markers to determine their maturation and activation status. As in wild-type controls, splenic B cells from ITAM mutants were $CD43^-$ and <20% of them stained brightly

Table I. *Relative Size of B Cell Fractions in BM and Spleen*

	BM (percentage of all cells)				
	Pro-B (A–C)	Pre-B (D)	Immature (E)	Recirculating (F)	Spleen ($\times 10^6$)
wt ($n = 9$)	2.4 ± 0.8	8.9 ± 3.0	5.4 ± 0.9	7.2 ± 2.4	27.7 ± 5.1
$Ig\alpha^{FF/FF}$ ($n = 8$)	3.0 ± 1.0	7.7 ± 2.3	5.8 ± 1.5	4.3 ± 1.7	23.0 ± 4.6
$Ig\alpha^{\Delta c/\Delta c}$ ($n = 5$)	5.0 ± 0.4	0.82 ± 0.18	0.54 ± 0.07	0.03 ± 0.01	0.21 ± 0.12
$Ig\beta^{\Delta c/\Delta c}$ ($n = 5$)	4.8 ± 1.7	4.7 ± 2.5	4.6 ± 2.2	0.22 ± 0.07	0.82 ± 0.61

Sizes of BM B cell fractions A to F are indicated as percentage of all live cells. The absolute number of splenic B cells is shown. Values represent the mean ± SD of the indicated number of analyzed mice.

for immature B cell marker 493 (data not shown). Normal surface expression of activation markers CD86 (B7.2), CD69 (data not shown), and MHC class II (Table II) was observed.

Like the $Ig\alpha^{\Delta c/\Delta c}$ mutant (21), $Ig\alpha^{FF/FF}$ mice displayed allelic exclusion at the IgH locus as verified by the analysis of IgH allotype heterozygous mutant animals (unpublished data).

Alterations of Surface Receptor Expression Levels in $Ig\alpha^{FF/FF}$ Mice. Although the lack of Igα ITAM phosphorylation apparently did not block the generation of a large pool of mature B cells, it caused changes in the surface level expression of BCR and several coreceptors. Fig. 2 C shows a comparison of the surface IgM levels in splenic B cells of wild-type, $Ig\beta^{\Delta c/\Delta c}$, and $Ig\alpha^{FF/FF}$ mice. In contrast to the extremely low surface IgM levels of B cells in $Ig\beta^{\Delta c/\Delta c}$ mice, the Igα ITAM mutation led to increased surface IgM levels. In general, B cells from various lymphoid organs carrying the $Ig\alpha^{FF}$ allele express on average more surface IgM and IgD than B cells from control mice (Fig. 2, and Table II). This applies also for B1 cells in the peritoneal cavity (Fig. 2 F, and Table II). Furthermore, we consistently observed slightly higher surface expression levels of CD19 (Fig. 2 C, and Table II) and lower surface levels of CD22 and B220 (Table II) in B cells obtained from $Ig\alpha^{FF/FF}$ compared with wild-type mice.

Reduction of Marginal Zone and B1 B Cell Populations. Are the differences in receptor expression levels sufficient to compensate for the Igα ITAM phosphorylation deficiency and to allow for the normal generation of all peripheral B cell subsets? Three different main B cell subpopulations have been described for the spleen: immature, follicular, and marginal zone (MZ) B cells. MZ B cells are large cells that are $CD21^{bright}CD23^{low}$ and $IgM^{high}IgD^{low}$. Analysis of $Ig\alpha^{FF/FF}$ mice revealed that this population was reduced to 5–25% of wild-type controls (Fig. 2 D).

In the peritoneal cavity, B cell numbers, mainly $CD5^+$ B1 cells, were drastically reduced in the Igα ITAM mutant mice (Fig. 2 F). B1 cells are phenotypically characterized as $IgM^{bright}IgD^{low}$ and express lower levels of surface B220. Most B1 cells are also $CD43^+$ and $CD23^-$. As shown in Fig. 2 F, this fraction of peritoneal B cells was reduced in $Ig\alpha^{FF/FF}$ mice and most remaining B cells resembled B2 cells in being $B220^{bright}$, IgD^+, $CD23^+$, and $CD43^-$. Corresponding to the reduction of B1 cell numbers, the T cell fraction ($CD5^+IgM^-$; Fig. 2 F) of peritoneal lymphocytes was increased.

Table II. *Comparison of Relative Expression Levels of Various B Cell Surface Molecules in Wild-Type and $Ig\alpha^{FF/FF}$ Mice*

Antigen	B cell population		Surface expression in $Ig\alpha^{FF/FF}$ mice relative to wild-type (% ± SD)		
IgM	BM	IgM^+B220^{low}	144.5 ± 35.0	$n = 10$	*
		IgM^+B220^{high}	248.2 ± 58.6	$n = 15$	**
	Spleen		205.5 ± 33.8	$n = 11$	**
	Blood		222.3 ± 13.9	$n = 5$	**
	Peritoneum	B1 cells	171.5 ± 37.8	$n = 8$	*
IgD	BM		126.9 ± 9.3	$n = 10$	**
	Spleen		132.6 ± 12.0	$n = 11$	**
	Blood		127.9 ± 17.7	$n = 5$	#
B220	BM	Pre-B	99.2 ± 5.4	$n = 4$	
		IgM^+B220^{low}	96.6 ± 5.4	$n = 10$	
		IgM^+B220^{high}	91.1 ± 6.0	$n = 12$	**
	Spleen		88.1 ± 6.9	$n = 12$	**
	Blood		86.2 ± 6.8	$n = 5$	#
CD19	Spleen		116.6 ± 5.9	$n = 15$	**
	Blood		122.9 ± 11.4	$n = 5$	*
	Peritoneum	B1 cells	117.7 ± 13.5	$n = 6$	#
CD22	Spleen		81.8 ± 4.8	$n = 10$	**
MHCII	Spleen		102.0 ± 28.8	$n = 5$	

The levels of surface expression were determined by comparing the mean fluorescence intensities between B cells of wild-type (set as 100%) and $Ig\alpha^{FF/FF}$ mice. Numbers represent the mean percentages (± SD) based on the number of indicated analyses. In each single analysis, samples from $Ig\alpha^{FF/FF}$ mutants and wild-type mice were analyzed in parallel. The significance of difference was tested with the paired Student's *t* test. Asterisks indicate the determined *P* values: $\#P < 0.05$; $^*P < 0.01$; $^{**}P < 0.001$.

Table III. *Fraction of λ1 Light Chain Expressing Spleen B Cells in Igα and Igβ Mutant Mice*

wt	4.8 ± 0.6%	$n = 13$
$Ig\alpha^{FF/FF}$	10.9 ± 3.1%	$n = 10$
$Ig\alpha^{\Delta c/\Delta c}$	22.1 ± 3.1%	$n = 7$
$Ig\alpha^{\Delta c/\Delta c}$	20.4 ± 5.8%	$n = 4$

The frequency of B cells expressing a λ1 light chain was determined by flow cytometry and is shown as percentage of all splenic B cells. Values represent the mean ± SD of the indicated numbers of mice.

Higher Percentage of λ1 Light Chain Expressing B Cells in Igα/Igβ Mutants. As in the BM of $Ig\alpha^{FF/FF}$ mice, all B cell fractions were present in normal numbers, the lack of Igα ITAM phosphorylation does not appear to impose a block in early B cell development (Table I). However, the impact of the ITAM mutation on the rearrangement and/or selection of Ig light chains is apparent from the distortion of the ratio of κ versus λ light chain expressing B cells. Compared with wild-type controls, $Ig\alpha^{FF/FF}$ mice possessed more λ1 light chain expressing B cells (Table III, and Fig. 2 E). This phenomenon could also be seen, and appeared even more pronounced, in the cytoplasmic truncation mutants of Igα and Igβ (Table III).

Reduced IgG1 Serum Levels and Impaired TD Immune Response in $Ig\alpha^{FF/FF}$ Mice. Altered BCR signaling in $Ig\alpha^{FF/FF}$ mice may also affect immune responsiveness. To check whether the ITAM mutation influences the basal levels of Ig titers, Ig isotypes were determined by ELISA in the sera of unimmmunized mice. As shown in Fig. 3 A, the total amount of serum Ig in $Ig\alpha^{FF/FF}$ mice, calculated as a sum of the individual isotypes, was comparable to controls. Although B1 cells are thought to be the main contributors of serum IgM, the reduction in B1 and MZ B cells in Igα ITAM mutants did not result in reduced serum IgM concentration. However, the serum concentration of IgG1 in $Ig\alpha^{FF/FF}$ mice was significantly lower than in wild-type controls.

To analyze humoral immune responses, we immunized $Ig\alpha^{FF/FF}$ mice with the TI type II (TI-II) antigen NP-Ficoll and TD antigen NP-CG. For two reasons we expected to see an impaired TI-II response. First, in $Ig\alpha^{\Delta c/\Delta c}$ mice, B cells with a cytoplasmic truncation of Igα were unable to mount a measurable response toward NP-Ficoll (21), and second, recent data suggest that MZ B cells are required for a normal TI-II response (33). However, the

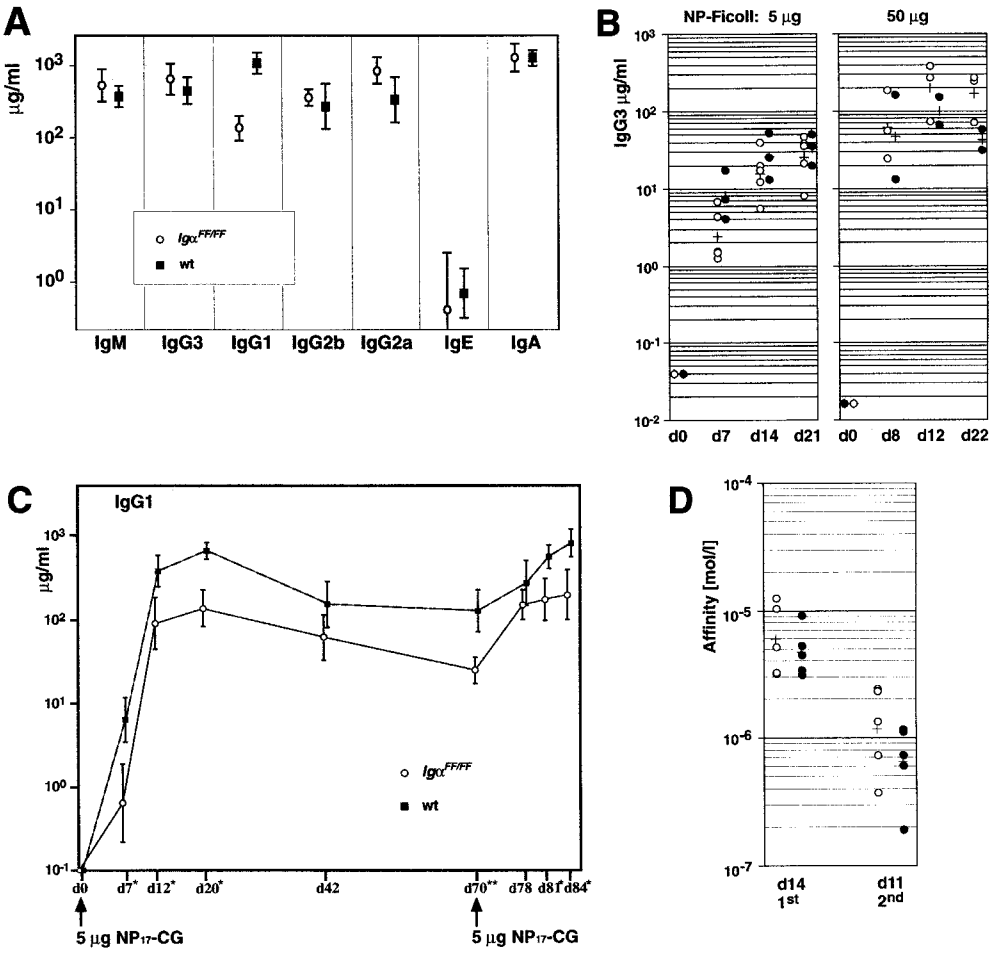

Figure 3. Serum Ig levels and humoral immune responses in $Ig\alpha^{FF/FF}$ mice. Serum Ig isotype levels were determined by ELISA. Filled symbols represent wild-type and open symbols represent $Ig\alpha^{FF/FF}$ mice. (A) Geometric means and standard deviations of serum levels of Igs in nonimmunized mice ($n = 5$). The data are representative of three independent analyses. (B) Immune response to TI-II NP-Ficoll antigen. Plots show NP-specific IgG3 in sera of mice after immunization with either 5 or 50 μg NP-Ficoll. Crosses indicate geometric mean values. (C) Immune response to a TD antigen. NP-specific IgG1 levels in primary and secondary responses after immunizations with 5 μg NP-CG were determined in $Ig\alpha^{FF/FF}$ mice ($n = 5$) and wild-type (wt) controls ($n = 6$). Shown are geometric mean values plus standard deviation. Asterisks indicate P values that were calculated according to the Student's t test. (D) Affinity maturation of anti-NP IgG1 in sera of $Ig\alpha^{FF/FF}$ and control mice. Affinities on day 14 after a primary and on day 11 after a secondary immunization with 5 μg NP-CG are shown.

NP-specific serum titers at different time points after the immunization revealed that Igα ITAM phosphorylation is not required for an efficient TI-II response (Fig. 3 B). *Igα*$^{FF/FF}$ mice were also able to mount primary and secondary TD responses, which had a kinetics comparable to those of wild-type controls (Fig. 3 C). These data imply that Igα ITAM phosphorylation is not a prerequisite for B cell memory formation. However, the TD response was significantly lower in *Igα*$^{FF/FF}$ mice at all time points examined (Fig. 3 C). To evaluate further the efficiency of the TD response, we determined the averaged relative affinity of the serum antibodies. Affinities of NP-specific antibodies were comparable between *Igα*$^{FF/FF}$ mice and control groups, and were equally increased in the course of the immune response, indicating effective affinity maturation (Fig. 3 D).

Stronger Calcium Response in Igα ITAM Mutant B Cells. To analyze the impact of the ITAM mutation on an early BCR-mediated signaling event, we stimulated Indo-1–loaded B cells either with F(ab)′$_2$ fragment of anti-Ig antibody or with anti-Ig antibodies and monitored changes in intracellular calcium by flow cytometry. Previously, we reported that a cytoplasmic truncation of Igα leads to an elevated and more sustained calcium response in immature B cells of *Igα*$^{\Delta c/\Delta c}$Ig^{HEL} mice compared with controls (23). We show here that this effect appears to be correlated with the phosphorylation of the Igα ITAM, as splenic B cells from *Igα*$^{FF/FF}$ mice also showed a stronger calcium response with a delayed maximum in comparison to wild-type controls (Fig. 4, and data not shown).

BCR Ligation Leads to Tyrosine Phosphorylation of Igα in Igα$^{FF/FF}$ *B Cells.* To extend the analysis of the signaling capacity of Igα ITAM mutant BCRs, we analyzed protein tyrosine phosphorylation after BCR cross-linking. Splenic B cells were isolated from *Igα*$^{FF/FF}$ and control mice, and stimulated with F(ab)′$_2$ fragment of anti-Ig antibody for different time durations. Total protein tyrosine phosphorylation was revealed by anti-phosphotyrosine immunoblotting. As shown in Fig. 5 A, BCRs lacking the Igα ITAM tyrosines were still capable of inducing protein tyrosine phosphorylation to levels comparable to controls. We then specifically examined the tyrosine phosphorylation of Igα and Igβ in anti-Igα immunoprecipitates before and after BCR cross-linking. As shown in Fig. 5 B, BCR ligation of *Igα*$^{FF/FF}$ B cells resulted in a rapid and persistent tyrosine phosphorylation of Igβ ITAM. Moreover, BCR-induced tyrosine phosphorylation of Igβ in *Igα*$^{FF/FF}$ mice was enhanced compared with controls (Fig. 5, A and B). Whereas Igβ possesses only the two tyrosines of its ITAM, the cytoplasmic tail of Igα contains four tyrosine residues (Fig. 1 E). Interestingly, Igα phosphorylation in Igα ITAM mutant B cells was detected after BCR ligation (Fig. 5 B). These data suggest that either one or both non-ITAM Igα tyrosine residues (#176 and #204) can be phosphorylated after

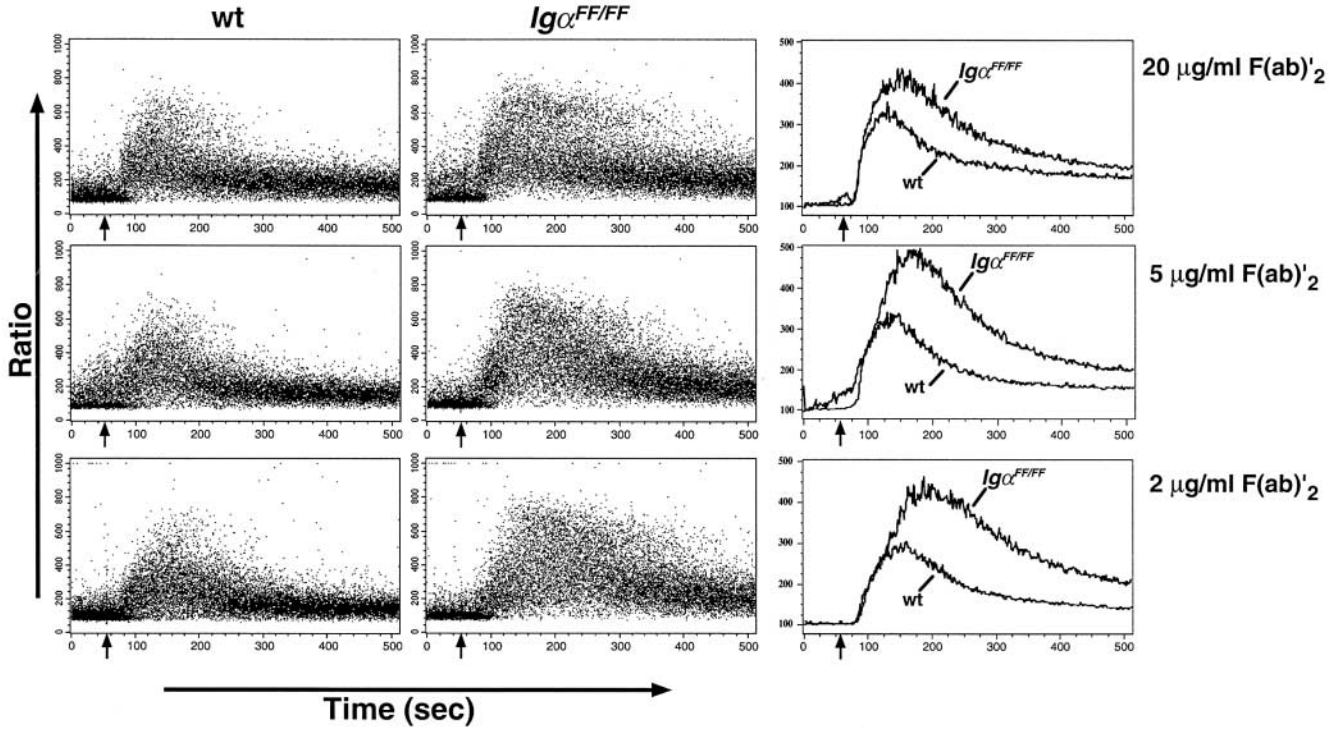

Figure 4. Comparison of BCR-induced Ca^{2+} mobilization. Changes in intracellular calcium levels were determined by flow cytometry. Dot plots present the intracellular calcium levels in B220$^+$ gated splenic B cells as the fluorescence ratio of Indo-1 emission at 395/510 nm recorded over time. Baseline fluorescence ratios were acquired for 50 s before F(ab)′$_2$ rabbit anti–mouse Ig antibodies were added (indicated by an arrow). Final antibody concentrations are shown on the right. Histograms on the right show the median values of the analyzed B cells. Results are representative of four independent experiments. wt, wild-type.

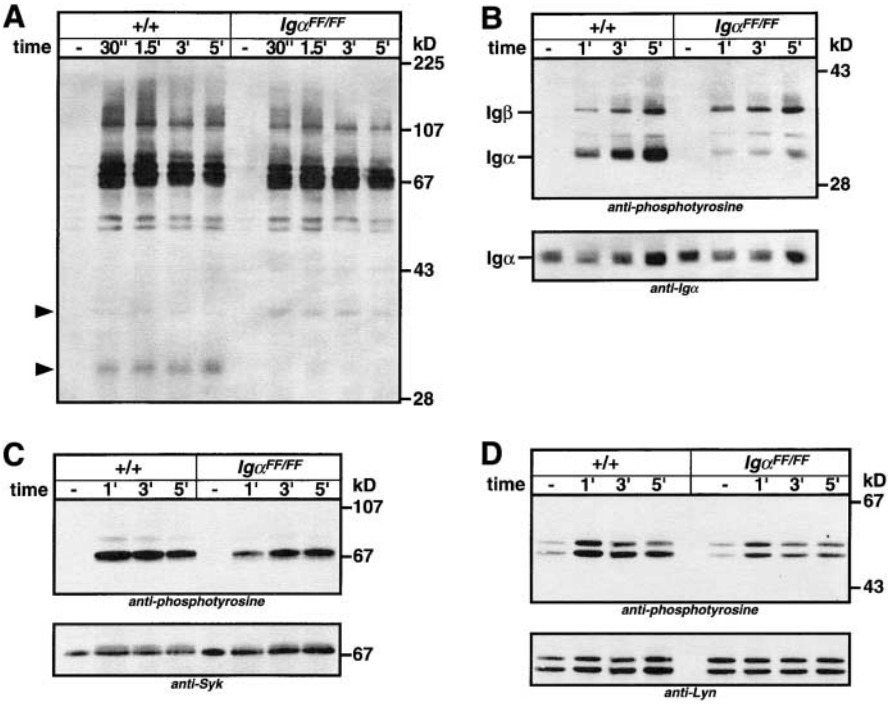

Figure 5. Analysis of protein tyrosine phosphorylation in splenic B cells of $Ig\alpha^{FF/FF}$ mice. Cell lysates of purified splenic B cells from $Ig\alpha^{FF/FF}$ and wild-type mice were prepared from cells that were either mock stimulated with medium or stimulated with 5 μg/10^6 cells $F(ab)'_2$ rabbit anti–mouse Ig for different periods of time. (A) Tyrosine phosphorylation of total cellular proteins (5×10^5 cells/lane) was detected by anti-phosphotyrosine immunoblotting. Arrows indicate the expected positions of Igα and Igβ. (B) Phosphotyrosine immunoblot of Igα immunoprecipitates. The bottom panel shows the same blot reprobed with an anti-Igα antibody. (C) Syk tyrosine phosphorylation. Proteins were immunoprecipitated from the cell lysates with anti-Syk antibody, resolved by SDS-PAGE, and analyzed by anti-phosphotyrosine immunoblotting. The blot was reprobed with anti-Syk antibody. (D) Phosphotyrosine immunoblot of Lyn immunoprecipitates. The blot was reprobed with anti-Lyn antibody.

BCR stimulation. This strongly suggests a role for the non-ITAM tyrosines in BCR-mediated signaling, e.g., as a binding site for SH2 domain containing proteins.

Syk kinase is one of the major signaling components that binds to doubly phosphorylated BCR ITAMs and becomes activated. Ligation of BCRs with the mutant Igα ITAM were still able to induce Syk tyrosine phosphorylation, presumably via phosphorylated Igβ. However, maximum phosphorylation was reached at a later time point than in wild-type controls (Fig. 5C). Examination of Lyn phosphorylation showed that basal tyrosine phosphorylation was similar between $Ig\alpha^{FF/FF}$ and wild-type B cells, but BCR-induced Lyn tyrosine phosphorylation was less than in wild-type controls (Fig. 5 D).

Complete Block of B Cell Development in $Ig\alpha^{FF/FF}Ig\beta^{\Delta c/\Delta c}$ Mice. Targeted mutations of Igα, as in truncation of the cytoplasmic tail in $Ig\alpha^{\Delta c/\Delta c}$ mice (21) or with specific loss of ITAM phosphorylation in $Ig\alpha^{FF/FF}$ mice, lead to alteration in development and responsiveness of B lymphocytes. Similarly, a cytoplasmic truncation of Igβ in $Ig\beta^{\Delta c/\Delta c}$ mice compromises B cell development and causes a strong reduction in mature B cells (22; Fig. 6). However, neither the lack of Igα nor Igβ ITAM alone leads to a complete block in B cell development. A cytoplasmic domain of either Igα or Igβ is still sufficient to signal (22). Based on the phenotypic differences between $Ig\alpha^{\Delta c/\Delta c}$ and $Ig\alpha^{FF/FF}$ mice and the finding that Igα may be phosphorylated at non-ITAM tyrosines, Igα may not mediate signaling exclusively through its phosphorylated ITAM. Whether development of B cells in the Igα and Igβ truncation mutants was absolutely dependent on the phosphorylation of the remaining BCR ITAM remained unclear. To answer this question, we generated $Ig\alpha^{FF/FF}Ig\beta^{\Delta c/\Delta c}$ mice. In comparison to $Ig\beta^{\Delta c/\Delta c}$ mice, the double mutants possessed no intact ITAM. As shown in Fig. 6 A, B cell development in these mice was completely blocked at the pro-B cell stage, as no $B220^+CD43^-$ B cells were present in the BM. FACS® analysis of the $B220^+CD43^+$ pro-B cell fraction revealed the presence of fractions A to C, but fraction C′ ($BP\text{-}1^+HSA^{bright}$) was absent (Fig. 6 B). In the periphery of $Ig\alpha^{FF/FF}Ig\beta^{\Delta c/\Delta c}$ mice, a few $CD19^+$ cells were still detectable (Fig. 6 C), however, these cells did not express surface IgM nor IgD. These $CD19^+$ cells expressed the immature B cell marker 493 and had low levels of surface CD19 and B220 (data not shown). Thus, these cells might represent peripheral B cell precursors. The lack of any functional mature B cells in $Ig\alpha^{FF/FF}Ig\beta^{\Delta c/\Delta c}$ mice was further validated by the absence of any detectable serum Igs (data not shown). Collectively, these data indicate an absolute requirement of Igα ITAM phosphorylation in $Ig\beta^{\Delta c/\Delta c}$ mice for B cells to develop beyond the pro-B cell stage.

Discussion

$Ig\alpha$ ITAM Mutation Affects B Cell Development Less Dramatically than Truncation of the $Ig\alpha$ Cytoplasmic Tail. The B cell antigen receptor complex relies on its Igα/Igβ heterodimer for surface expression, internalization, antigen presentation, and signaling. Therefore, a targeted ablation of the cytoplasmic effector domain of either Igα or Igβ may result in impaired B cell development and function. This is indeed evident in both $Ig\alpha^{\Delta c/\Delta c}$ and $Ig\beta^{\Delta c/\Delta c}$ mice which exhibit a drastic reduction in peripheral B cell numbers (21, 22). To date, the main signaling function of the Igα/Igβ heterodimer has been ascribed to its two ITAMs.

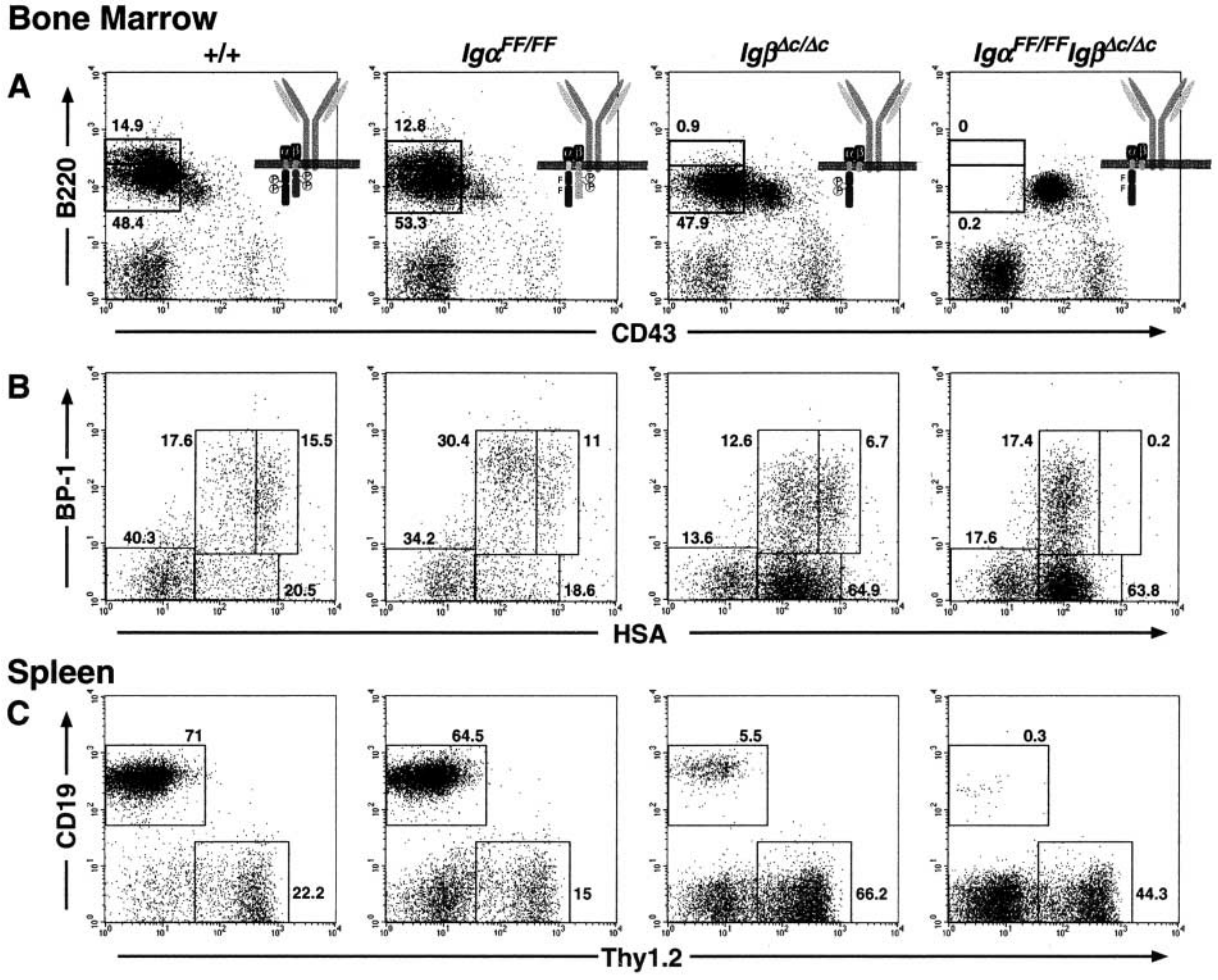

Figure 6. Complete block of B cell development at the pro-B cell stage in the absence of any phosphorylatable BCR ITAM. Representative flow cytometric analyses of lymphocytes from wild-type, $Ig\alpha^{FF/FF}$, $Ig\beta^{\Delta c/\Delta c}$, and $Ig\alpha^{FF/FF}Ig\beta^{\Delta c/\Delta c}$ mice. (A) Note the lack of $CD43^-$ B cells in the BM of $Ig\alpha^{FF/FF}$ $Ig\beta^{\Delta c/\Delta c}$ mice. (B) The HSA vs. BP-1 dot plots show $CD43^+B220^+$ gated pro-B cells. Numbers indicate the frequency of cells within the windows as percentage of the displayed pro-B cells. (C) CD19 and Thy1.2 surface expression of splenic lymphocytes. Fractions of B and T cells are shown as percentage of cells in the lymphocyte gate.

Moreover, mutational experiments in cell lines have revealed that ITAM functions require phosphorylation at its two tyrosine residues (9, 10, 13, 14, 16, 34). However, the present analysis of $Ig\alpha^{FF/FF}$ mice revealed striking differences in comparison to $Ig\alpha^{\Delta c/\Delta c}$ mice. A lack of Igα ITAM phosphorylation did not affect the relative fraction sizes of pro-B, pre-B, and immature B cells in the BM, and the absolute splenic B cell numbers in $Ig\alpha^{FF/FF}$ mice were comparable to those of wild-type controls. Taken together, the differences in phenotypes resulting from either the loss of the Igα cytoplasmic tail or the specific lack of Igα ITAM phosphorylation, imply a role for the non-phosphorylated ITAM and/or other parts of the Igα cytoplasmic tail in Igα-mediated function. This idea is consistent with the finding that Igα ITAM phosphorylation is not a prerequisite for binding of Src family kinases Lyn and Fyn via their N-terminal regions (35) and in agreement with the model that proposes a high affinity, phosphotyrosine-dependent, and a low affinity, phosphotyrosine-independent association of Src family kinases with Igα/Igβ (36). In addition, the Igα molecules in $Ig\alpha^{\Delta c/\Delta c}$ mice lack the serine/threonine phosphorylation sites which are implicated in the regulation of Igα tyrosine phosphorylation (37). Thus, differences in serine/threonine phosphorylation might also be responsible for the phenotypic differences of $Ig\alpha^{\Delta c/\Delta c}$ and $Ig\alpha^{FF/FF}$ mice. Alternatively, lack of the Igα cytoplasmic domain in $Ig\alpha^{\Delta c/\Delta c}$ mice might influence the structure of the remaining Igβ tail and distort its ITAM function. The different phenotype of $Ig\alpha^{FF/FF}$ mice could thus also reflect a difference in Igβ ITAM function.

Altered Surface Antigen Expression in B Cells of $Ig\alpha^{FF/FF}$ Mice Due to Adaptation or Selection. B cells from $Ig\alpha^{FF/FF}$ mice express higher levels of surface IgM and IgD compared with wild-type controls. Three reasons might account for the higher BCR density. First, lack of efficient protein-kinase activation via phosphorylated Igα ITAMs might be partly compensated by expressing more Igα/Igβ on the cell surface. Second, the increase in Igβ ITAM phosphorylation

might partially substitute for the lack of Igα ITAM phosphorylation. Third, Igα ITAM phosphorylation might directly control BCR surface expression or internalization. The latter possibility is supported by the analysis of Igα mutant molecules in cell cultures. While in reconstitution experiments using the J558Lμm cell line, neither a cytoplasmic deletion nor Ig−ITAM tyrosine mutations interfered with the surface expression of BCR (10), constitutive receptor endocytosis appeared to be dependent on the cytoplasmic tail of Igα in a chimeric system (38). Similarly, analyzing FcγRII-Igα or Igβ chimeric molecules in the A20/IIA1.6 cell line, efficient constitutive BCR internalization was only mediated by the cytoplasmic domain of Igα and was shown to be dependent on the first Igα ITAM tyrosine (38).

Interestingly, B cells in $Ig\alpha^{\Delta c/\Delta c}$ mice do not exhibit a similar increase in surface BCR expression levels as in $Ig\alpha^{FF/FF}$ mice, and the cytoplasmic truncation of Igβ in $Ig\beta^{\Delta c/\Delta c}$ mice leads to lowered BCR expression (22; Fig. 2, B and C). One might speculate that surface BCR expression levels are controlled by constitutive Igα/Igβ-dependent turnover mechanisms and in addition are adjusted to the specific signaling requirements of the B cells.

In line with the idea that Igα ITAM phosphorylation is required for efficient activation of Src family kinases are the observations of an increased CD19 and a decreased CD22 coreceptor surface expression in B cells from $Ig\alpha^{FF/FF}$ mice. CD19 was shown to lower the threshold of BCR-mediated cell activation and to be involved in the activation of Src family kinases (39, 40). In contrast, CD22 contains immunoreceptor tyrosine-based inhibitory motifs (ITIMs) which serve as docking sites for SH2 domain-containing phosphotyrosine phosphatase (SHP)-1, and thus might serve to lower protein kinase activity (41–43). Interestingly, B cells in CD22-deficient mice (44, 45) and transgenic mice overexpressing CD19 (46) possess decreased surface IgM levels. Thus, differences in BCR and coreceptor surface expression levels in $Ig\alpha^{FF/FF}$ mice might be the result of selection and/or adaptation of B cells, in an attempt to cope with weakened intrinsic BCR signaling. To address the issue of selection versus adaptation, we plan to analyze $Ig\alpha^{FF\text{-}flox/FF\text{-}flox}$ mice in combination with inducible or developmental stage specific Cre-recombinase expression (47). The floxed Igα allele (Fig. 1 A, 4) allows undisturbed B cell development with a wild-type BCR until Cre-mediated mutation of the Igα ITAM occurs. Induced mutagenesis should thus allow us to study the adaptive response of mature B cells to a lack of Igα ITAM phosphorylation.

PTK Activation by Igα ITAM and Non-ITAM Tyrosine Phosphorylation. Previous studies with B cell lines have implied a critical requirement for Igα ITAM tyrosine phosphorylation in the activation of PTKs after BCR ligation (9, 10, 13, 48). However, in some initial signaling studies with splenic B cells of $Ig\alpha^{FF/FF}$ mice we did not observe a drastic reduction in overall protein tyrosine phosphorylation after BCR cross-linking, which could be explained by the presence of a functional Igβ ITAM. Overall higher surface expression and more efficient ITAM phosphorylation of Igβ might thus be able to compensate in part for the lack of Igα ITAM phosphorylation in $Ig\alpha^{FF/FF}$ B cells. We tested the capability of Syk and Lyn to undergo tyrosine phosphorylation upon BCR ligation in B cells of $Ig\alpha^{FF/FF}$ mice. Although Igα ITAM phosphorylation is not absolutely required to induce tyrosine phosphorylation of Syk, the overall Syk tyrosine phosphorylation was lower and delayed as a result of the Igα ITAM mutation. Similarly, Lyn was inducibly tyrosine phosphorylated in $Ig\alpha^{FF/FF}$ B cells, but to a lesser extent than in controls. An important novel finding is the demonstration of Igα tyrosine phosphorylation apart from its ITAM. This suggests an involvement of the Igα non-ITAM tyrosines in BCR-dependent signaling. These might recruit distinct signaling proteins or alternatively enhance or inhibit the association of molecules with the Igα/Igβ heterodimer. Both non-ITAM tyrosines are indeed in the sequence context of a potential Src family SH2 domain binding site (49, 50). Compared with wild-type controls, the weak tyrosine phosphorylation of Igα in $Ig\alpha^{FF/FF}$ B cells supports the idea that the ITAM tyrosines are the main tyrosine phosphorylation sites in Igα (10). However, in the wild-type situation, phosphorylation of the non-ITAM tyrosines could well be linked to and dependent on Igα ITAM phosphorylation. A clarification of these matters will require a biochemical analysis which is beyond the scope of this paper.

Igα ITAM Phosphorylation and Ca^{2+} Mobilization. The enhanced Ca^{2+}-flux in B cells of $Ig\alpha^{FF/FF}$ mice after BCR ligation seems to contradict the idea that Igα ITAM phosphorylation functions to amplify signaling. Previous transfection experiments with FcγRII-Igα or FcγRII-Igβ chimeric molecules in the IIA1.6 cell line demonstrated that only the Igα cytoplasmic tail was capable to mobilize Ca^{2+} from intracellular stores and influx of extracellular calcium. In contrast, the Igβ cytoplasmic domain stimulated only an oscillatory release from intracellular stores, which overall resulted in a small increase of free intracellular Ca^{2+} (9, 51). Further analyses specified an absolute requirement of the proximal Igα ITAM tyrosine (Y182) for Ca^{2+} mobilization (9, 13). Thus, it was surprising to find an even stronger Ca^{2+} mobilization in splenic B cells of $Ig\alpha^{FF/FF}$ mice after BCR ligation (Fig. 4). One might interpret the data such that Igα ITAM phosphorylation is required to contain and terminate Ca^{2+} mobilization. While the increased Ca^{2+} mobilization in B cells of $Ig\alpha^{FF/FF}$ mice is not caused by overall higher surface BCR expression (data not shown), changes of coreceptor expression might influence the outcome of BCR ligation by resetting signaling thresholds. In support of the latter, overexpression of CD19 (46) or lack of CD22 (44, 45, 52, 53) in mouse B cells also leads to enhanced calcium mobilization, whereas the lack of CD19 lowers it (54).

Igα/Igβ Mutations Distort Light Chain Rearrangements. Although we do not yet know whether the Igα ITAM mutation leads to enhanced editing of autoreactive BCRs like the Igα truncation (23), it is noteworthy that both mutations distort the κ to λ ratio in favor of λ light chain expression. One might speculate that quantitative and qualita-

tive alterations of signals transmitted by a mutant Igα/Igβ complex might hinder the efficient termination of light chain rearrangements in B cell development, widening the time window in which sequential rearrangements in the light chain loci occur and thus driving more cells to the λ chain expression, if κ rearrangements usually preceed λ rearrangements (55). In line with this interpretation are the observations that the shift in favor of λ chain expression is more pronounced in the tail truncation mutants than in *Igα*$^{FF/FF}$ mice and that only in the former mutants there is an apparent block of B cell development at the immature B cell stage. Alternatively, altered pre-BCR signaling might influence the order of light chain gene rearrangements and cause an earlier opening of the λ locus. In an extreme scenario this could lead to the exclusive rearrangement of the λ locus in λ chain–expressing cells. We tested this hypothesis by analyzing the rearrangement status of the κ loci in λ1$^+$ splenic B cells. However, similar to the situation in λ1$^+$ cells from wild-type mice (56), the κ light chain loci were found to be rearranged in λ1$^+$ cells of *Igα*$^{FF/FF}$ mice (data not shown). Finally, it might be possible that λ light chains confer a selective advantage for B cells in case of distorted BCR signaling.

Dependence of B1 and MZ B Cell Populations on Igα ITAM Phosphorylation. In the peritoneal cavity of *Igα*$^{FF/FF}$ mice, the total number of B cells was lower than in the wild-type due to a drastic reduction in B1a cells. The majority of the remaining peritoneal B cells were phenotypically B2 cells. B1 cells often express germline-encoded self-reactive BCRs and appear to have signaling requirements that are different from B2 cells (57). Recent studies have demonstrated that the expression of an autoreactive receptor can drive the generation of B1 cells (58, 59), suggesting that B1 cell development depends on signals mediated by BCR–ligand interaction. The specific reduction of B1 cells in *Igα*$^{FF/FF}$ mice could thus be explained by enhanced negative selection of autoreactive BCR specificities, but would also be consistent with the idea that Igα ITAM phosphorylation functions as a signal amplifier. In support of the latter conclusion, several mouse mutants affecting genes involved in positive regulation of BCR signaling such as CD19 (60, 61), Btk (62, 63), and Vav (64, 65) also show a reduction in the B1 cell population. An opposing phenotype is seen upon mutation of genes thought to negatively regulate BCR-related signaling. SHP-1 deficiency in *me*^{v}/me^{v} mice (66) and knockouts of CD22 (53, 45) and CD72 (67) all lead to an expansion of the B1 cell population. This is also true for mice in which the SHP-1 gene is selectively inactivated in B cells (data not shown).

In the spleen of *Igα*$^{FF/FF}$ mice we observed a strong reduction of MZ B cells. Similar to the B1 population, MZ B cell selection also depends on BCR specificities with a bias for autoreactivity (68). Moreover, both B1 and MZ B cells are CD23^{low}IgM^{high} and larger in size than B2 cells. Theses results demonstrate directly that appropriate BCR signaling is required for the normal generation and maintenance of both these subsets.

Igα ITAM Phosphorylation Is Required for Efficient TD Immune Responses. B1 and MZ B cells are thought to be the frontline of an early defense against pathogens and appear to be regulated in a T cell–independent way (69). In a recent study of Pyk-2 knockout mice, which completely lack MZ B cells, an important role for MZ B cells in T cell–independent antibody responses was suggested (33). Therefore and because TI-II responses have been shown to be severely impaired in Igα and Igβ tail truncation mutants (21, 22), we expected an impairment of the anti-NP-Ficoll response in *Igα*$^{FF/FF}$ mice. However, the selective elimination of the Igα ITAM does apparently not interfere with efficient B cell activation upon strong BCR cross-linking. It is unclear at this point whether the difference between the Igα ITAM and the truncation mutants in this respect reflects a difference in B cell activation or relates to the development of B cell subsets which may be disturbed in the mutants to different extents. That the Igα ITAM mutation is compatible with an intact TI-II response, but affects the efficiency of a TD antibody response is consistent with the findings in cell lines that Igα ITAM tyrosines contribute to efficient antigen presentation, but are not absolutely required for the presentation of multivalent antigens (48, 70, 71). Inefficient TD responses may also explain the low IgG1 levels in the sera of *Igα*$^{FF/FF}$ mice.

Absolute Requirement of BCR ITAM Tyrosines for B Cell Development Beyond the Pro-B Cell Stage. A striking observation is the absolute block of B cell development at the pro-B cell stage in mice lacking the Igα ITAM and the Igβ cytoplasmic tail. This contrasts with an almost unimpaired early B cell development in the Igα ITAM mutant and significant pre-B cell promotion in mice expressing a truncated Igβ or Igα chain. The simplest interpretation of these results is that there is significant functional redundancy between the Igα and Igβ ITAM (similar to that exhibited by the ITAMs of the T cell receptor complex; reference 72), and that there is an absolute requirement for the presence of an ITAM in the pre-BCR at the pro- to pre-B cell transition which is known from earlier work to depend on pre-BCR expression (17, 29, 73–75). It remains to be established whether this requirement relates to pre-BCR surface expression or more likely, the signaling function of the surface bound receptor. The latter aspect is supported by previous findings showing a requirement of ITAM tyrosines for pre-B cell development and allelic exclusion in transgenic systems using IgM/Igβ and IgM/Igα chimeric receptors (18–20). It will be interesting to determine whether later stages of B cell development, where the BCR rather than the pre-BCR plays a critical role (21, 76–78), exhibit a similar ITAM dependence. Inducible targeted mutagenesis will be instrumental in resolving this issue.

We thank Dr. H. Singh for the genomic cosmid clone and Dr. A. Rolink for the monoclonal antibody 493. We are grateful to A. Egert, C. Göttlinger, G. Ringeisen, A. Leinhaas, C. Uthoff-Hachenberg, and S. Willms for excellent technical help, and to Dr. Raul Torres and members of the Rajewsky lab for discussion and support.

This work was supported by the Volkswagen Foundation (grant no. I/71768), the Deutsche Forschungsgemeinschaft through SFB 243, the European Community (grant no. BIO4-CT96-0077), the Alexander von Humboldt Foundation to L. Pao, and by the Max-Planck Research Award to K. Rajewsky.

Submitted: 18 April 2001
Revised: 12 June 2001
Accepted: 21 June 2001

References

1. Healy, J.I., and C.C. Goodnow. 1998. Positive versus negative signaling by lymphocyte antigen receptors. *Annu. Rev. Immunol.* 16:645–670.
2. Rajewsky, K. 1996. Clonal selection and learning in the antibody system. *Nature.* 381:751–758.
3. Schamel, W.W., and M. Reth. 2000. Monomeric and oligomeric complexes of the B cell antigen receptor. *Immunity.* 13:5–14.
4. Reth, M. 1989. Antigen receptor tail clue. *Nature.* 338:383–384.
5. Benschop, R.J., and J.C. Cambier. 1999. B cell development: signal transduction by antigen receptors and their surrogates. *Curr. Opin. Immunol.* 11:143–151.
6. Rudd, C.E. 1999. Adaptors and molecular scaffolds in immune cell signaling. *Cell.* 96:5–8.
7. Clark, M.R., K.S. Campbell, A. Kazlauskas, S.A. Johnson, M. Hertz, T.A. Potter, C. Pleiman, and J.C. Cambier. 1992. The B cell antigen receptor complex: association of Ig-alpha and Ig-beta with distinct cytoplasmic effectors. *Science.* 258: 123–126.
8. Johnson, S.A., C.M. Pleiman, L. Pao, J. Schneringer, K. Hippen, and J.C. Cambier. 1995. Phosphorylated immunoreceptor signaling motifs (ITAMs) exhibit unique abilities to bind and activate Lyn and Syk tyrosine kinases. *J. Immunol.* 155: 4596–4603.
9. Cassard, S., D. Choquet, W.H. Fridman, and C. Bonnerot. 1996. Regulation of ITAM signaling by specific sequences in Ig-beta B cell antigen receptor subunit. *J. Biol. Chem.* 271: 23786–23791.
10. Flaswinkel, H., and M. Reth. 1994. Dual role of the tyrosine activation motif of the Ig-alpha protein during signal transduction via the B cell antigen receptor. *EMBO J.* 13:83–89.
11. Kim, K.M., G. Alber, P. Weiser, and M. Reth. 1993. Differential signaling through the Ig-alpha and Ig-beta components of the B cell antigen receptor. *Eur. J. Immunol.* 23:911–916.
12. Luisiri, P., Y.J. Lee, B.J. Eisfelder, and M.R. Clark. 1996. Cooperativity and segregation of function within the Ig-alpha/beta heterodimer of the B cell antigen receptor complex. *J. Biol. Chem.* 271:5158–5163.
13. Pao, L.I., S.J. Famiglietti, and J.C. Cambier. 1998. Asymmetrical phosphorylation and function of immunoreceptor tyrosine- based activation motif tyrosines in B cell antigen receptor signal transduction. *J. Immunol.* 160:3305–3314.
14. Sanchez, M., Z. Misulovin, A.L. Burkhardt, S. Mahajan, T. Costa, R. Franke, J.B. Bolen, and M. Nussenzweig. 1993. Signal transduction by immunoglobulin is mediated through Ig alpha and Ig beta. *J. Exp. Med.* 178:1049–1055.
15. Taddie, J.A., T.R. Hurley, B.S. Hardwick, and B.M. Sefton. 1994. Activation of B- and T-cells by the cytoplasmic domains of the B-cell antigen receptor proteins Ig-alpha and Ig-beta. *J. Biol. Chem.* 269:13529–13535.
16. Williams, G.T., C.J. Peaker, K.J. Patel, and M.S. Neuberger. 1994. The alpha/beta sheath and its cytoplasmic tyrosines are required for signaling by the B-cell antigen receptor but not for capping or for serine/threonine-kinase recruitment. *Proc. Natl. Acad. Sci. USA.* 91:474–478.
17. Gong, S., and M.C. Nussenzweig. 1996. Regulation of an early developmental checkpoint in the B cell pathway by Ig beta. *Science.* 272:411–414.
18. Papavasiliou, F., M. Jankovic, H. Suh, and M.C. Nussenzweig. 1995. The cytoplasmic domains of immunoglobulin (Ig) alpha and Ig beta can independently induce the precursor B cell transition and allelic exclusion. *J. Exp. Med.* 182:1389–1394.
19. Papavasiliou, F., Z. Misulovin, H. Suh, and M.C. Nussenzweig. 1995. The role of Ig beta in precursor B cell transition and allelic exclusion. *Science.* 268:408–411.
20. Teh, Y.M., and M.S. Neuberger. 1997. The immunoglobulin (Ig)alpha and Igbeta cytoplasmic domains are independently sufficient to signal B cell maturation and activation in transgenic mice. *J. Exp. Med.* 185:1753–1758.
21. Torres, R.M., H. Flaswinkel, M. Reth, and K. Rajewsky. 1996. Aberrant B cell development and immune response in mice with a compromised BCR complex. *Science.* 272:1802–1804.
22. Reichlin, A., Y. Hu, E. Meffre, H. Nagaoka, S. Gong, M. Kraus, K. Rajewsky, and M.C. Nussenzweig. 2001. B cell development is arrested at the immature B cell stage in mice carrying a mutation in the cytoplasmic domain of immunoglobulin β. *J. Exp. Med.* 193:13–24.
23. Kraus, M., K. Saijo, R.M. Torres, and K. Rajewsky. 1999. Ig-alpha cytoplasmic truncation renders immature B cells more sensitive to antigen contact. *Immunity.* 11:537–545.
24. Torres, R.M., and K. Hafen. 1999. A negative regulatory role for Ig-alpha during B cell development. *Immunity.* 11: 527–536.
25. Thomas, K.R., and M.R. Capecchi. 1987. Site-directed mutagenesis by gene targeting in mouse embryo-derived stem cells. *Cell.* 51:503–512.
26. Feldhaus, A.L., D. Mbangkollo, K.L. Arvin, C.A. Klug, and H. Singh. 1992. BLyF, a novel cell-type- and stage-specific regulator of the B-lymphocyte gene mb-1. *Mol. Cell. Biol.* 12:1126–1133.
27. Torres, R.M., and R. Kühn. 1997. Laboratory Protocols for Conditional Gene Targeting. Oxford University Press, Oxford. 167 pp.
28. Schwenk, F., U. Baron, and K. Rajewsky. 1995. A cre-transgenic mouse strain for the ubiquitous deletion of loxP-flanked gene segments including deletion in germ cells. *Nucleic Acids Res.* 23:5080–5081.
29. Gu, H., Y.R. Zou, and K. Rajewsky. 1993. Independent control of immunoglobulin switch recombination at individual switch regions evidenced through Cre-loxP-mediated gene targeting. *Cell.* 73:1155–1164.
30. Roes, J., and K. Rajewsky. 1993. Immunoglobulin D (IgD)-deficient mice reveal an auxiliary receptor function for IgD in antigen-mediated recruitment of B cells. *J. Exp. Med.* 177: 45–55.
31. Cumano, A., and K. Rajewsky. 1986. Structure of primary anti-(4-hydroxy-3-nitrophenyl)acetyl(NP) antibodies in normal and idiotypically suppressed C57Bl/6 mice. *Eur. J. Immunol.* 15:512.
32. Hardy, R.R., C.E. Carmack, S.A. Shinton, J.D. Kemp, and K. Hayakawa. 1991. Resolution and characterization of

pro-B and pre-pro-B cell stages in normal mouse bone marrow. *J. Exp. Med.* 173:1213–1225.
33. Guinamard, R., M. Okigagi, J. Schlessinger, and J.V. Ravetch. 2000. Absence of marginal zone B cells in Pyk-2-deficient mice defines their role in the humoral response. *Nat. Immunol.* 1:31–36.
34. Letourneur, F., and R.D. Klausner. 1992. Activation of T cells by a tyrosine kinase activation domain in the cytoplasmic tail of CD3 epsilon. *Science.* 255:79–82.
35. Pleiman, C.M., C. Abrams, L.T. Gauen, W. Bedzyk, J. Jongstra, A.S. Shaw, and J.C. Cambier. 1994. Distinct p53/56lyn and p59fyn domains associate with nonphosphorylated and phosphorylated Ig-alpha. *Proc. Natl. Acad. Sci. USA.* 91: 4268–4272.
36. Clark, M.R., S.A. Johnson, and J.C. Cambier. 1994. Analysis of Ig-alpha-tyrosine kinase interaction reveals two levels of binding specificity and tyrosine phosphorylated Ig-alpha stimulation of Fyn activity. *EMBO J.* 13:1911–1919.
37. Müller, R., J. Wienands, and M. Reth. 2000. The serine and threonine residues in the Ig-alpha cytoplasmic tail negatively regulate immunoreceptor tyrosine- based activation motif-mediated signal transduction. *Proc. Natl. Acad. Sci. USA.* 97: 8451–8454.
38. Cassard, S., J. Salamero, D. Hanau, D. Spehner, J. Davoust, W.H. Fridman, and C. Bonnerot. 1998. A tyrosine-based signal present in Ig alpha mediates B cell receptor constitutive internalization. *J. Immunol.* 160:1767–1773.
39. Carter, R.H., and D.T. Fearon. 1993. CD19: lowering the threshold for antigen receptor stimulation of B lymphocytes. *Science.* 256:105–107.
40. Fujimoto, M., Y. Fujimoto, J.C. Poe, P.J. Jansen, C.A. Lowell, A.L. DeFranco, and T.F. Tedder. 2000. CD19 regulates Src family protein tyrosine kinase activation in B lymphocytes through processive amplification. *Immunity.* 13:47–57.
41. Campbell, M.A., and N.R. Klinman. 1995. Phosphotyrosine-dependent association between CD22 and protein tyrosine phosphatase 1C. *Eur. J. Immunol.* 25:1573–1579.
42. Doody, G.M., L.B. Justement, C.C. Delibrias, R.J. Matthews, J. Lin, M.L. Thomas, and D.T. Fearon. 1995. A role in B cell activation for CD22 and the protein tyrosine phosphatase SHP. *Science.* 269:242–244.
43. Law, C.L., S.P. Sidorenko, K.A. Chandran, Z. Zhao, S.H. Shen, E.H. Fischer, and E.A. Clark. 1996. CD22 associates with protein tyrosine phosphatase 1C, Syk, and phospholipase C-gamma(1) upon B cell activation. *J. Exp. Med.* 183: 547–560.
44. Otipoby, K.L., K.B. Andersson, K.E. Draves, S.J. Klaus, A.G. Farr, J.D. Kerner, R.M. Perlmutter, C.L. Law, and E.A. Clark. 1996. CD22 regulates thymus-independent responses and the lifespan of B cells. *Nature.* 384:634–637.
45. Sato, S., A.S. Miller, M. Inaoki, C.B. Bock, P.J. Jansen, M.L. Tang, and T.F. Tedder. 1996. CD22 is both a positive and negative regulator of B lymphocyte antigen receptor signal transduction: altered signaling in CD22-deficient mice. *Immunity.* 5:551–562.
46. Zhou, L.J., H.M. Smith, T.J. Waldschmidt, R. Schwarting, J. Daley, and T.F. Tedder. 1994. Tissue-specific expression of the human CD19 gene in transgenic mice inhibits antigen-independent B-lymphocyte development. *Mol. Cell. Biol.* 14: 3884–3894.
47. Kühn, R., F. Schwenk, M. Aguet, and K. Rajewsky. 1995. Inducible gene targeting in mice. *Science.* 269:1427–1429.
48. Siemasko, K., B.J. Eisfelder, C. Stebbins, S. Kabak, A.J. Sant, W. Song, and M.R. Clark. 1999. Ig alpha and Ig beta are required for efficient trafficking to late endosomes and to enhance antigen presentation. *J. Immunol.* 162:6518–6525.
49. Payne, G., L.A. Stolz, D. Pei, H. Band, S.E. Shoelson, and C.T. Walsh. 1994. The phosphopeptide-binding specificity of Src family SH2 domains. *Chem. Biol.* 2:99–105.
50. Songyang, Z., S.E. Shoelson, M. Chaudhuri, G. Gish, T. Pawson, W.G. Haser, F. King, T. Roberts, S. Ratnofsky, R.J. Lechleider, et al. 1993. SH2 domains recognize specific phosphopeptide sequences. *Cell.* 72:767–778.
51. Choquet, D., G. Ku, S. Cassard, B. Malissen, H. Korn, W.H. Fridman, and C. Bonnerot. 1994. Different patterns of calcium signaling triggered through two components of the B lymphocyte antigen receptor. *J. Biol. Chem.* 269:6491–6497.
52. Nitschke, L., R. Carsetti, B. Ocker, G. Kohler, and M.C. Lamers. 1997. CD22 is a negative regulator of B-cell receptor signalling. *Curr. Biol.* 7:133–143.
53. O'Keefe, T.L., G.T. Williams, S.L. Davies, and M.S. Neuberger. 1996. Hyperresponsive B cells in CD22-deficient mice. *Science.* 274:798–801.
54. Buhl, A.M., C.M. Pleiman, R.C. Rickert, and J.C. Cambier. 1997. Qualitative regulation of B cell antigen receptor signaling by CD19: selective requirement for PI3-kinase activation, inositol-1,4,5-trisphosphate production and $Ca2^+$ mobilization. *J. Exp. Med.* 186:1897–1910.
55. Engel, H., A. Rolink, and S. Weiss. 1999. B cells are programmed to activate kappa and lambda for rearrangement at consecutive developmental stages. *Eur. J. Immunol.* 29:2167–2176.
56. Zou, Y.R., S. Takeda, and K. Rajewsky. 1993. Gene targeting in the Ig kappa locus: efficient generation of lambda chain-expressing B cells, independent of gene rearrangements in Ig kappa. *EMBO. J.* 12:811–820.
57. Hayakawa, K., and R.R. Hardy. 2000. Development and function of B-1 cells. *Curr. Opin. Immunol.* 12:346–353.
58. Chumley, M.J., J.M. Dal Porto, S. Kawaguchi, J.C. Cambier, D. Nemazee, and R.R. Hardy. 2000. A VH11V kappa 9 B cell antigen receptor drives generation of $CD5^+$ B cells both in vivo and in vitro. *J. Immunol.* 164:4586–4593.
59. Hayakawa, K., M. Asano, S.A. Shinton, M. Gui, D. Allman, C.L. Stewart, J. Silver, and R.R. Hardy. 1999. Positive selection of natural autoreactive B cells. *Science.* 285:113–116.
60. Engel, P., L.J. Zhou, D.C. Ord, S. Sato, B. Koller, and T.F. Tedder. 1995. Abnormal B lymphocyte development, activation, and differentiation in mice that lack or overexpress the CD19 signal transduction molecule. *Immunity.* 3:39–50.
61. Rickert, R.C., K. Rajewsky, and J. Roes. 1995. Impairment of T-cell-dependent B-cell responses and B-1 cell development in CD19-deficient mice. *Nature.* 376:352–355.
62. Kerner, J.D., M.W. Appleby, R.N. Mohr, S. Chien, D.J. Rawlings, C.R. Maliszewski, O.N. Witte, and R.M. Perlmutter. 1995. Impaired expansion of mouse B cell progenitors lacking Btk. *Immunity.* 3:301–312.
63. Khan, W.N., F.W. Alt, R.M. Gerstein, B.A. Malynn, I. Larsson, G. Rathbun, L. Davidson, S. Muller, A.B. Kantor, L.A. Herzenberg, et al. 1995. Defective B cell development and function in Btk-deficient mice. *Immunity.* 3:283–299.
64. Tarakhovsky, A., M. Turner, S. Schaal, P.J. Mee, L.P. Duddy, K. Rajewsky, and V.L. Tybulewicz. 1995. Defective antigen receptor-mediated proliferation of B and T cells in the absence of Vav. *Nature.* 374:467–470.
65. Zhang, R., F.W. Alt, L. Davidson, S.H. Orkin, and W. Swat. 1995. Defective signalling through the T- and B-cell antigen

receptors in lymphoid cells lacking the vav proto-oncogene. *Nature*. 374:470–473.
66. Cyster, J.G., and C.C. Goodnow. 1995. Protein tyrosine phosphatase 1C negatively regulates antigen receptor signaling in B lymphocytes and determines thresholds for negative selection. *Immunity*. 2:13–24.
67. Pan, C., N. Baumgarth, and J.R. Parnes. 1999. CD72-deficient mice reveal nonredundant roles of CD72 in B cell development and activation. *Immunity*. 11:495–506.
68. Martin, F., and J.F. Kearney. 2000. Positive selection from newly formed to marginal zone B cells depends on the rate of clonal production, CD19, and btk. *Immunity*. 12:39–49.
69. Fagarasan, S., and T. Honjo. 2000. T-independent immune response: new aspects of B cell biology. *Science*. 290:89–92.
70. Lankar, D., V. Briken, K. Adler, P. Weiser, S. Cassard, U. Blank, M. Viguier, and C. Bonnerot. 1998. Syk tyrosine kinase and B cell antigen receptor (BCR) immunoglobulin-alpha subunit determine BCR-mediated major histocompatibility complex class II–restricted antigen presentation. *J. Exp. Med*. 188:819–831.
71. Patel, K.J., and M.S. Neuberger. 1993. Antigen presentation by the B cell antigen receptor is driven by the alpha/beta sheath and occurs independently of its cytoplasmic tyrosines. *Cell*. 74:939–946.
72. Ardouin, L., C. Boyer, A. Gillet, J. Trucy, A.M. Bernard, J. Nunes, J. Delon, A. Trautmann, H.T. He, B. Malissen, and M. Malissen. 1999. Crippling of CD3-zeta ITAMs does not impair T cell receptor signaling. *Immunity*. 10:409–420.
73. Kitamura, D., J. Roes, R. Kühn, and K. Rajewsky. 1991. A B cell-deficient mouse by targeted disruption of the membrane exon of the immunoglobulin mu chain gene. *Nature*. 350:423–426.
74. Mombaerts, P., J. Iacomini, R.S. Johnson, K. Herrup, S. Tonegawa, and V.E. Papaioannou. 1992. RAG-1-deficient mice have no mature B and T lymphocytes. *Cell*. 68:869–877.
75. Shinkai, Y., G. Rathbun, K.P Lam, E.M. Oltz, V. Stewart, M. Mendelsohn, J. Charron, M. Datta, F. Young, A.M. Stall, et al. 1992. RAG-2-deficient mice lack mature lymphocytes owing to inability to initiate V(D)J rearrangement. *Cell*. 68: 855–867.
76. Lam, K.P., R. Kühn, and K. Rajewsky. 1997. In vivo ablation of surface immunoglobulin on mature B cells by inducible gene targeting results in rapid cell death. *Cell*. 90:971–973.
77. Spanopoulou, E., C.A. Roman, L.M. Corcoran, M.S. Schlissel, D.P. Silver, D. Nemazee, M.C. Nussenzweig, S.A. Shinton, R.R. Hardy, and D. Baltimore. 1994. Functional immunoglobulin transgenes guide ordered B-cell differentiation in Rag-1-deficient mice. *Genes. Dev*. 8:1030–1042.
78. Young, F., B. Ardman, Y. Shinkai, R. Lansford, T.K. Blackwell, M. Mendelsohn, A. Rolink, F. Melchers, and F.W. Alt. 1994. Influence of immunoglobulin heavy- and light-chain expression on B-cell differentiation. *Genes. Dev*. 8:1043–1057.